J Fluoresc (2011) 21:487–495
DOI 10.1007/s10895-010-0735-9

ORIGINAL PAPER

Binding of an Anti-inflammatory Drug Lornoxicam with Blood Proteins: Insights from Spectroscopic Investigations

Reeta Punith · Ashwini H. Hegde · Seetharamappa Jaldappagari

Received: 2 July 2010 / Accepted: 28 September 2010 / Published online: 6 October 2010

Abstract The interaction between an anti-inflammatory drug, lornoxicam (LXM) and protein (human serum albumin and bovine serum albumin) was studied by spectroscopic techniques (Fluorescence, synchronous, FT-IR, UV-vis absorption and circular dichroism). The quenching mechanism of fluorescence of the protein by the drug was discussed. Based on the interaction studies carried out at different temperatures by spectrofluorometry, the binding constant and the number of binding sites for drug on protein have been evaluated. The nature of binding force operating between the drug and protein was proposed to be electrostatic and hydrophobic based on thermodynamic parameters. The distance r between the donor (protein) and acceptor (drug) was determined based on the Förster's theory of non-radiation energy transfer and found to be 2.38 nm and 2.56 nm for LXM-BSA and LXM-HSA respectively. Displacement studies with different site probes revealed that the drug bound to the hydrophobic pocket located in sub domain IIA; that is to say, Trp-214 was near or within the binding site. Circular dichroism data of protein in the presence of drug revealed the decreased α-helicity and hence changes in secondary structure of protein. The effects of some common ions were also investigated.

Keywords Protein · Lornoxicam · Quenching · Binding characteristics · Spectroscopic investigations

This paper was presented at "Fluorescence 2009", an International Conference of Fluorescence in Biology, held at Tata Institute of Fundamental Research (TIFR), Mumbai, India, during 16–19th March 2009.

R. Punith · A. H. Hegde · S. Jaldappagari (✉)
Department of Chemistry, Karnatak University,
Dharwad 580 003, India
e-mail: jseetharam@yahoo.com

Introduction

Lornoxicam (LXM) is a non-steroidal anti-inflammatory drug (Fig. 1) of the oxicam class with analgesic, anti-inflammatory and antipyretic properties. It is available in oral and parenteral formulations. It is used for inflammatory disease of the joints, osteoarthritis, pain following surgery and pain in the lower back and hip which travels down the back of the thigh into the leg (sciatica). LXM differs from other oxicam compounds in its potent inhibition of prostaglandin biosynthesis, a property that explains the particularly pronounced efficacy of the drug.

Serum albumins, human serum albumin (HSA) and bovine serum albumin (BSA) are the most common soluble proteins in the body of all the vertebrates and HSA is the most prominent protein in the plasma [1]. It binds to a wide variety of substances like metals, fatty acids, amino acids, hormones and a large list of drugs. The formed complexes between protein and the ligands are involved in transport and regulatory processes [2]. BSA shows 76% structural homology with HSA [3] and it differs from HSA in the polypeptide chain having 582 amino acid residues whereas HSA has 585 amino acid residue monomers. Both serum proteins are divided into three linearly arranged, structurally distinct and evolutionarily related domains I, II and III. Each domain can be classified into two subdomains, A and B possessing common structural motifs [4]. HSA consists of a single Tryptophan residue, Trp-214 that invariably appears in hydrophobic cavity of subdomain IIA, while the BSA consists of two Tryptophans embedded in two different domains (Trp-134 is located in proximity of the protein surface, but buried in a hydrophobic pocket of domain IIA and Trp-214 is located in internal part of domain IIIA) [5].

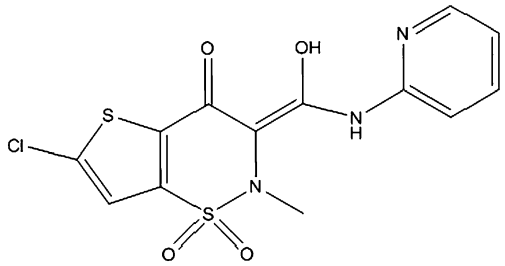

Fig. 1 Structure of LXM

The mechanism of interaction between a drug and plasma protein can influence the protein structure and functions and hence is of crucial importance for us to understand the pharmacodynamics and pharmacokinetics of the drug. Several studies on fluorescence quenching and mechanism of interaction between drugs or other bioactive small molecules and albumin have been reported [6–10]. Therefore, the knowledge of the study carries an enormous biological interest and is helpful for the design of new drugs [11]. So, this kind of study is expected to provide salient information of the structural features that determine the therapeutic effectiveness of the drug and hence become an important research field in chemistry, life sciences and clinical medicine. Hence, it was thought worthwhile to investigate the detailed mechanism of interaction of an anti-inflammatory drug, LXM with proteins employing different spectroscopic techniques.

Experimental Details

Apparatus

Fluorescence measurements were performed on a spectro-fluorimeter Model F-2000 (Hitachi, Japan) equipped with a 150W Xenon lamp and a slit width of 5 nm. A 1 cm quartz cell was used for measurements. The CD measurements were made on a JASCO-J-715 spectropolarimeter (Tokyo, Japan) using a 0.1 cm cell at 0.2 nm intervals, with 3 scans averaged for each CD spectrum in the range of 200–260 nm. The absorption spectra were recorded on a double beam CARY 50-BIO UV-visible spectrophotometer (Varian, Australia) equipped with a 150 W Xenon lamp and a slit width of 5 nm. A quartz cell of 1 cm was used for measurements. FT-IR spectra were recorded on Nicolet Nexus 670 FT-IR spectrometer (USA) equipped with a Germanium attenuated total reflection (ATR) accessory, a DTGS KBr detector and a KBr beam splitter.

Reagents

BSA (fatty acid free, Fraction V) HSA (fatty acid free) were obtained from Sigma Chemical Company, St. Louis, USA. LXM was obtained as a gift sample from Greece. The solutions of BSA and HSA were prepared in 0.1 M phosphate buffer of pH 7.4 containing 0.15 M NaCl. BSA and HSA solutions were prepared based on their molecular weight of 65,000 and 66,000 respectively. The LXM was prepared in 12% DMSO. All other materials employed were of analytical reagent grade and millipore water was used throughout.

Procedure

LXM-BSA/HSA Interactions

On the basis of preliminary experiments, fluorescence spectra were recorded in the range of 300–500 nm and 280–500 nm for BSA and HSA respectively. BSA/HSA concentration was kept fixed at 1.237 μM and that of drug was varied from 1.237 μM to 10.321 μM.

Thermodynamics of Drug-Protein Interactions

Thermodynamic parameters for the binding of drug to BSA/HSA were determined by carrying out the binding studies at three different temperatures, 289, 294 and 299 K in the range of 300–500 nm upon excitation at 296/280 nm by spectrofluorimetric method.

The Displacement Experiments

The displacement experiments were performed using the site probes by keeping the concentration of BSA/HSA and the probe, constant (each of 1.237 μM). The fluorescence quenching studies were carried out as before to determine the binding constants of LXM-BSA/HSA system in presence of the site probes, warfarin, ibuprofen and digitoxin for sites I, II and III, respectively.

Circular Dichroism (CD) Measurements

The CD measurements of BSA/HSA (125 μM) in the presence and absence of LXM were made in the range of 200–260 nm. The BSA/HSA to drug concentration was varied in the ratio of 1:1, 1:4 and 1:8 and the CD spectra were recorded.

UV-Visible Absorption Studies

The absorption spectra of BSA/HSA in the presence and absence of LXM were recorded in the range of 230–330 nm. BSA and HSA concentrations were fixed at 1.237 μM while that of the drug was varied from 1.237 μM to 10.321 μM.

Fourier Transform Infrared Spectroscopy

All spectra were taken via the attenuated total reflection (ATR) method with a resolution of 4 cm^{-1} and using 60 scans. The spectra processing procedure involved collecting spectra of the buffer solution under the same conditions. Next, the absorbance of the buffer solution was subtracted from the spectrum of the sample solution to obtain the FT-IR spectrum of the protein.

Synchronous Fluorescence Measurements

The fluorescence studies were carried out on a RF-5301PC spectrofluorimeter (Shimadzu). The spectra were recorded in the range of 280–400 nm. The synchronous fluorescence spectra were recorded with scanning ranges, $\Delta\lambda$ =15 nm and 60 nm ($\Delta\lambda = \lambda_{em} - \lambda_{ex}$) in the absence and in the presence of LXM, to know the spectrum characteristic of protein residues.

Energy Transfer Between NAP and Protein

The absorption spectrum of drug (1.237 μM) in the range of 300–450 nm and the emission spectrum of protein (1.237 μM) were recorded in the range of 280–450 nm. Then, the overlap of the UV absorption spectrum of drug with the fluorescence emission spectrum of protein was utilized to evaluate the energy transfer.

Effects of Some Common Ions

The fluorescence spectra of LXM-protein were recorded in presence and absence of various common ions *viz*., K^+, Ca^{2+}, Cu^{2+} and Zn^{2+} upon excitation at 296/280 nm. The overall concentration of protein and common ion was fixed at 1.237 μM.

Results and Discussion

Fluorescence Quenching Mechanism

Fluorescence quenching refers to any process which decreases the fluorescence intensity of a sample [12]. A variety of molecular interactions can result in quenching including excited-state reactions, molecular rearrangements, energy transfer, ground-state complex formation and collisional quenching. The fluorescence quenching spectra of BSA/HSA with increasing concentrations of LXM are shown in Fig. 2a and b, by fixing excitation wavelength at 296 and 280 nm for BSA and HSA, respectively. BSA/HSA exhibited strong fluorescence emission while LXM did not show intrinsic fluorescence under the experimental conditions. The fluorescence intensity of BSA/HSA decreased regularly and a very slight blue shift was observed for the emission wavelength with increase in concentration of LXM, indicating the formation of a drug-protein complex [13]. Different mechanisms of quenching are usually classified as either dynamic quenching or static quenching. Dynamic and static quenching can be distinguished by their differing dependence on temperature and viscosity [14]. Dynamic quenching depends upon diffusion. Since higher temperatures result in larger diffusion coefficients, the bimolecular quenching constants are expected to increase with increase in temperature. In contrast, increased temperature is likely to result in decreased stability of complexes, and thus lower values of quenching rate constants are observed for the static quenching [15]. In order to speculate the fluorescence quenching mechanism, the fluorescence quenching data at different temperatures (289, 294 and 299 K) were firstly analyzed using the classical Stern-Volmer equation [16].

$$\frac{F_0}{F} = 1 + K_{sv}[Q] \quad (1)$$

where F_0 and F are the fluorescence intensities in the absence and presence of quencher, respectively, $[Q]$ is the concentration of quencher and K_{sv} is the Stern-Volmer quenching constant, which was obtained by plotting F_0/F *versus* $[Q]$

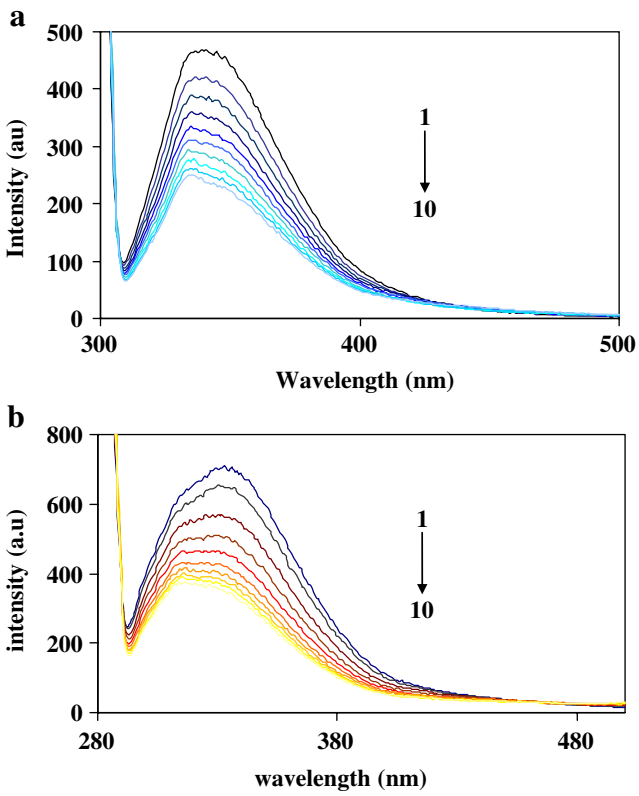

Fig. 2 Fluorescence spectra of (**a**) BSA and (**b**) HSA in presence of LXM. Concentration of BSA/HSA was fixed at 1.237 μM (1) and that of LXM was maintained in the range of 1.237–10.321 μM (2–10)

(Fig. 3a and b). The results shown in Table 1 indicated that the K_{sv} values are directly correlated with temperature suggesting the presence of dynamic collision mechanism in the interaction of LXM with protein.

Binding Parameters

The binding constant (K) and the number of binding sites (n) can be calculated using the equation shown below:

$$\log(F_0 - F)/F = \log K + n \log[Q] \quad (2)$$

A plot of log $[(F_0\text{-}F)/F]$ *versus* log $[Q]$ gives a straight line, whose slope equals to n and the intercept on Y-axis equals to log K. The values of K and n at 289, 294 and 299 K are listed in Table 2. The results indicate that there is one class of binding site for LXM in BSA/HSA. The fact that the binding constant between LXM and BSA/HSA increased with increasing temperature suggested that there was strong interaction between LXM and BSA/HSA [17]. This clearly implied that LXM would be bound, stored and transported by BSA/HSA in the body.

Site Probe Studies

Sudlow et al. [18] have proposed that the biding sites on protein are sites I and II. Site I has affinity for warfarin, phenylbutazone, etc. and site II for ibuprofen, flufenamic acid, etc. It is reported that digitoxin binding is independent of sites I and II [19, 20] and binds to site III. Competitive binding studies were performed using site probes, warfarin, ibuprofen, and digitoxin for site I, II and III respectively. For this, emission spectra of ternary mixture of LXM-BSA-site probe and LXM-HSA-site probe were recorded, separately. The corresponding binding constants were found to be as 1.581×10^2, 1.724×10^3 and 1.751×10^3 $M^{-1}$for site I, II and III respectively for LXM-BSA and 2.35×10^2, $2{,}63\times10^3$ and 2.67×10^3 M^{-1} for site I, II and III respectively for LXM-HSA. As evident from the above values, the LXM was not significantly displaced by ibuprofen or digitoxin. However, warfarin (site I) showed a significant displacement of LXM in both BSA and HSA suggesting that LXM binding site on protein is site I. Hence, the site I located in subdomain II A near Trp-214 is proposed to be the main binding site for LXM in BSA/HSA.

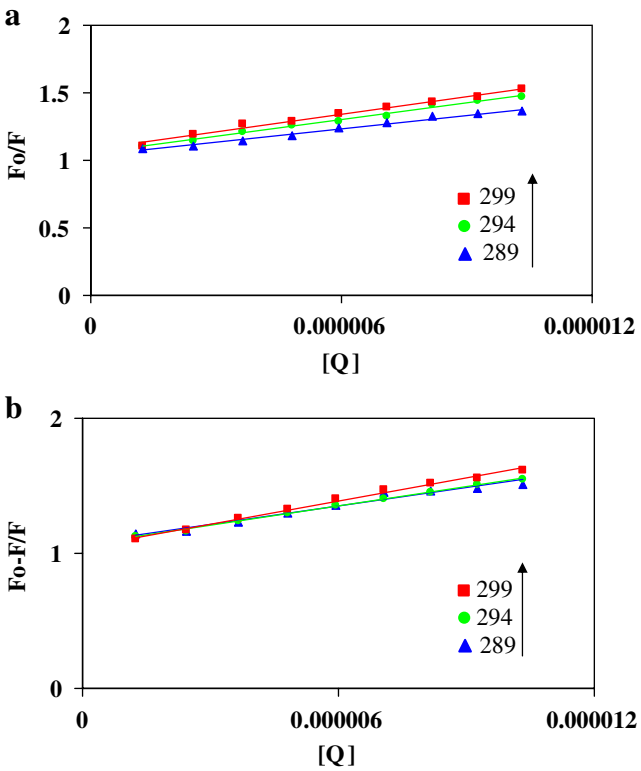

Fig. 3 The Stern-Volmer curves for quenching of (**a**) BSA and (**b**) HSA with LXM at (♦) 289 (▲) 294 and (●) 299 K

Determination of the Force Acting Between LXM and BSA/HSA

Ligands bind to protein essentially by four main types of non-covalent interactions *viz;* hydrogen bonds, van der Waals forces, hydrophobic and electrostatic interactions. The binding forces are characterized and confirmed by analyzing thermodynamic parameters dependent on temperatures [21]. The thermodynamic parameters were calculated using the van't Hoff equation shown below:

$$\log K = \frac{-\Delta H^0}{2.303RT} + \frac{\Delta S^0}{2.303R} \quad (3)$$

where K is the associative binding constant, ΔH^0 is the change in enthalpy, ΔS^0 is the change in entropy and R is the gas constant. The ΔH^0 and ΔS^0 are obtained from the slope and ordinates of the plot of log K *versus* $1/T$. The free energy change (ΔG^0) is estimated from the following relationship:

$$\Delta G^0 = -2.303RT \log K \quad (4)$$

Positive enthalpy (ΔH^0) and positive entropy (ΔS^0) values of the interaction of LXM with BSA/HSA indicated that the hydrophobic interactions played a major role in the interaction [22]. Negative ΔG^0 values revealed the spontaneity of binding process.

CD Spectroscopy Studies

CD spectroscopy is one of the best methods for examining the conformational changes of proteins whose secondary structure may vary in accordance with their bound state. The CD spectra of BSA/HSA exhibit two negative bands in

Table 1 Stern-Volmer quenching constants for the interactions of LXM with BSA and HSA at different temperatures

	T (K)	K_{sv} (L mol^{-1})	R^2
BSA	289	3.2952×10^4	0.9856
	294	4.1448×10^4	0.9880
	299	4.3621×10^4	0.9885
HSA	289	4.5159×10^4	0.9726
	294	4.7551×10^4	0.9965
	299	5.6402×10^4	0.9947

the ultraviolet region at 208 and 220 nm. When various concentrations of LXM were added to free protein, the intensity at 208 and 220 nm decreased (Fig. 4a and b) in a concentration dependant manner [23]. This indicated the considerable changes in the protein secondary structure. Specifically, it suggested the loss of α-helical stability, which might be the result of the formation of a complex between the protein and LXM. The CD results were expressed in terms of mean residue ellipticity (MRE) in degree cm^{2}dmol^{-1} according to following equation:

$$\mathrm{MRE} = \frac{\text{Observed CD (m degree)}}{C_p n l \times 10} \quad (5)$$

where C_p is the molar concentration of the protein, n is the number of amino acid residues and l is the path length. The helical content of the free and combined BSA were calculated from MRE values at 208 using the equation shown below [24]:

$$\alpha\text{-helix}(\%) = \frac{[\mathrm{MRE}_{208} - 4000]}{[33000 - 4000]} \times 100 \quad (6)$$

where MRE_{208} is the observed MRE value at 208 nm, 4000 is the MRE of the α-form and random coil conformation cross at 208 nm and 33,000 is the MRE value of a pure α-helix at 208 nm. From the above equation, α-helicity in the secondary structure of BSA/HSA was determined. In free BSA and HSA, the secondary structure consisted of 60.07% and 58.62% of α-helices respectively under experimental conditions. The proportions of secondary structural elements undergo marginal variation at low

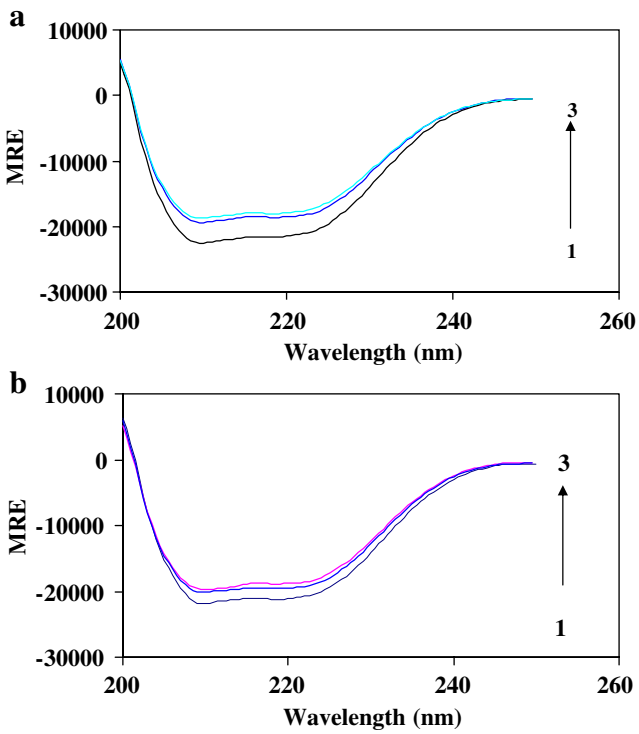

Fig. 4 CD spectra of (**a**) BSA and (**b**) HSA [(1)1.237 μM] in presence of (2) 4.948 and (3) 9.896 μM LXM

concentrations of LXM. However, with increase in addition of LXM, there was a significant change in protein conformation. At 1:8 ratio of protein to LXM concentration, the α-helical stability was decreased to 47.94% and 51.26% in BSA and HSA, respectively. This was attributed to the changes in the amino acid residue of the main polypeptide chain of protein and destruction of its hydrogen bonding networks [25].

UV-Vis Absorption Studies

UV-visible absorption spectra of BSA/HSA without and with varying concentration of LXM were obtained by subtracting corresponding buffer (Fig. 5a and b). The spectra of protein in the presence of increasing concentration of drug showed the increase in absorbance values with blue shift in λ_{max} from 275 nm to 270 nm. The results

Table 2 Binding constant and thermodynamic parameters of LXM-BSA and LXM-HSA interactions

Drug	T (K)	K (L mol^{-1})	n	R^2	ΔH^0 (kJ/mol)	ΔG^0 (kJ/mol)	ΔS^0 (J/mol/K)
BSA	289	1.571×10^3	0.9310	0.9612	+21.262	−17.47	+134
	294	1.622×10^3	0.9483	0.9203		−18.14	
	299	2.114×10^3	0.9238	0.9929		−18.80	
HSA	289	1.348×10^3	0.9849	0.9629	+137.23	−17.09	+534
	294	2.526×10^3	0.9377	0.9885		−19.77	
	299	9.136×10^3	0.9357	0.9973		−22.44	

indicated that there exists interaction between LXM and BSA/HSA led to ground state complex formation and change in the microenvironment around BSA/HSA [26].

FT-IR Spectra of LXM-BSA/HSA

Infrared spectroscopy has long been used as a simple and powerful method for investigating the secondary structure of proteins. In the IR region, the frequencies of bands due to the amide I and II vibrations are sensitive to the secondary structure of proteins. The amide I vibration mode originates from the C=O stretching vibration of the amide group and gives rise to infrared bands in the region between approximately 1600 cm^{-1} and 1700 cm^{-1}. The amide II band at 1550 cm^{-1} originates from the C-N stretching coupled with N-H bending modes [27]. The spectra of free protein (only protein solution) and bound protein [(protein solution + drug solution) - (drug solution)] were obtained in order to monitor the intensity variations of these vibrations.

In case of BSA, amide I band was shifted from 1629.58 cm^{-1} to 1639.23 cm^{-1} and amide II band was shifted from 1550.12 cm^{-1} to 1556.22 cm^{-1} (Figure not shown) and in case of HSA, amide I band was shifted from 1638.19 cm^{-1} to 1641.12 cm^{-1} and amide II band was shifted from 1538.91 cm^{-1} to 1558.2 cm^{-1} (Figure not shown) respectively upon interaction with drug. These results indicated that the addition of LXM caused a change in the protein secondary structure upon complexation [28].

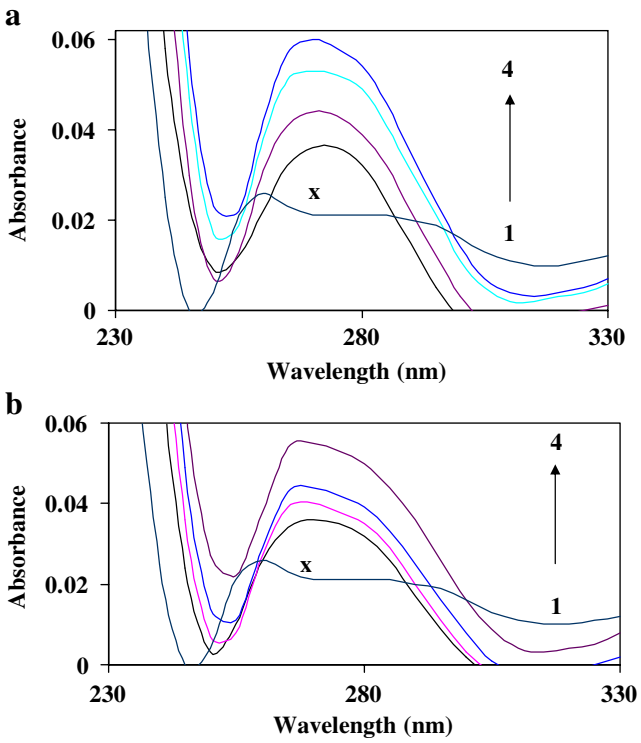

Fig. 5 Absorption spectra of (**a**) BSA and (**b**) HAS [(1) 1.237 μM] in presence of (2) 1.237 μM (3) 5.952 μM and (4) 10.321 μM, LXM. A concentration of 1.237 μM (x) was used for LXM only

Characteristics of Synchronous Fluorescence Method

Synchronous fluorescence spectra can provide the information on the molecular microenvironment, particularly in the vicinity of the fluorophore molecules. The excitation and emission monochromators are synchronously scanned, separated by a constant wavelength interval $\Delta\lambda$ ($\Delta\lambda = \lambda_{em}-\lambda_{ex}$). When $\Delta\lambda$=15 nm, the spectrum characteristic of the protein tyrosine (Tyr) residues was observed, and when $\Delta\lambda$=60 nm, the spectrum characteristic of protein tryptophan (Trp) residues was observed [29]. The fluorescence emission peak for aromatic Tyr and Trp residues are sensitive to the polarity of their environment. The red shift signifies that the fluorescing aromatic residues buried in nonpolar hydrophobic cavities are moved to a more hydrophilic environment; on the contrary, the blue shift suggests an increase of hydrophobicity [30].

To study the conformational change in the protein, the possible shift in the wavelength emission maximum λ_{max} for Tyr and Trp residues was measured by scanning synchronously at $\Delta\lambda$=15 nm and $\Delta\lambda$=60 nm. The concentration of protein was kept constant and was progressively titrated with LXM by gradually increasing its concentration. This led to a dramatic decrease in the fluorescence intensity of Tyr and Trp residues of BSA/HSA and no shift for Tyr and Trp residues of BSA/HSA was observed (Figs. 6 and 7) indicating that the binding between LXM and the protein did not lead to a change in the polarity of the microenvironment of the Tyr and Trp residues, but the internal packing of the protein changed [31].

Energy Transfer Between LXM and BSA/HSA

The overlap of UV-visible absorption spectrum of LXM with the fluorescence emission spectrum of BSA and HSA is shown in Fig. 8a and b, respectively. According to the Förster's non-radiative energy transfer theory [32], the efficiency of energy transfer depends on

(i) the extent of overlap between the donor emission and the acceptor absorption spectrum,
(ii) the orientation of the transition dipole of donor and acceptor and
(iii) the distance between the donor and the acceptor.

Here, the donor and acceptor are BSA/HSA and LXM, respectively. The efficiency of energy transfer (E) is given by:

$$E = 1 - \frac{F}{F_0} = \frac{R_0^6}{R_0^6 + r^6} \quad (7)$$

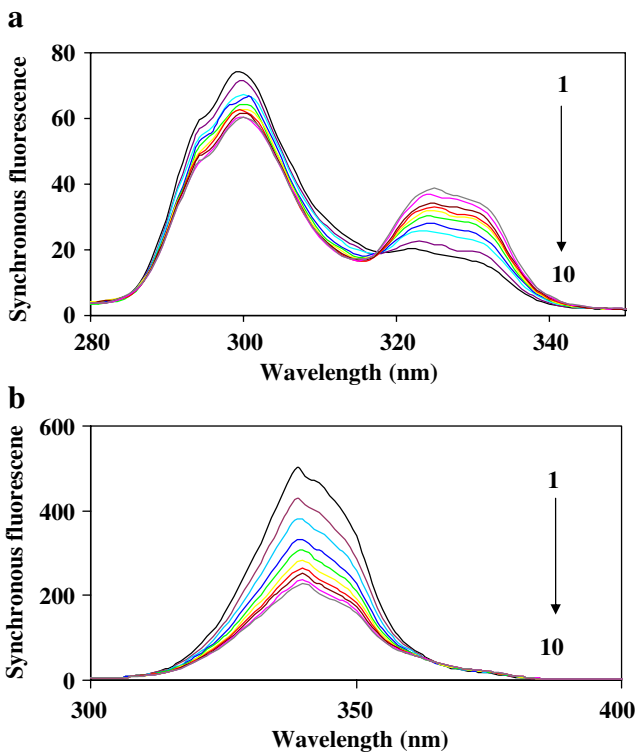

Fig. 6 Synchronous fluorescence spectra of BSA with various amounts of LXM: (**a**) Δλ=15 nm and (**b**) Δλ=60 nm; [BSA] = 1.237 μM (1); 2–10 corresponding to [LXM] =1.237–10.321 μM

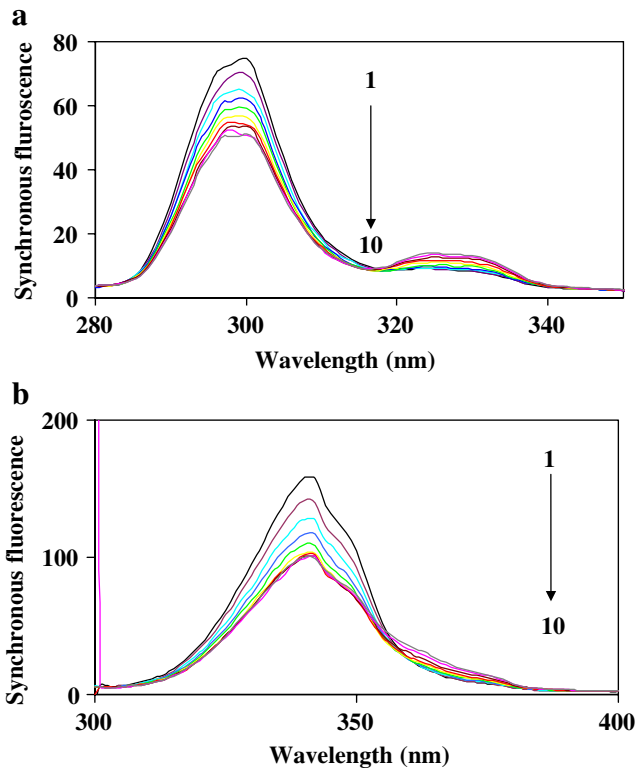

Fig. 7 Synchronous fluorescence spectra of HSA with various amounts of LXM: (**a**) Δλ=15 nm and (**b**) Δλ=60 nm; [HSA] = 1.237 μM (1); 2–10 corresponding to [LXM] =1.237- 10.321 μM

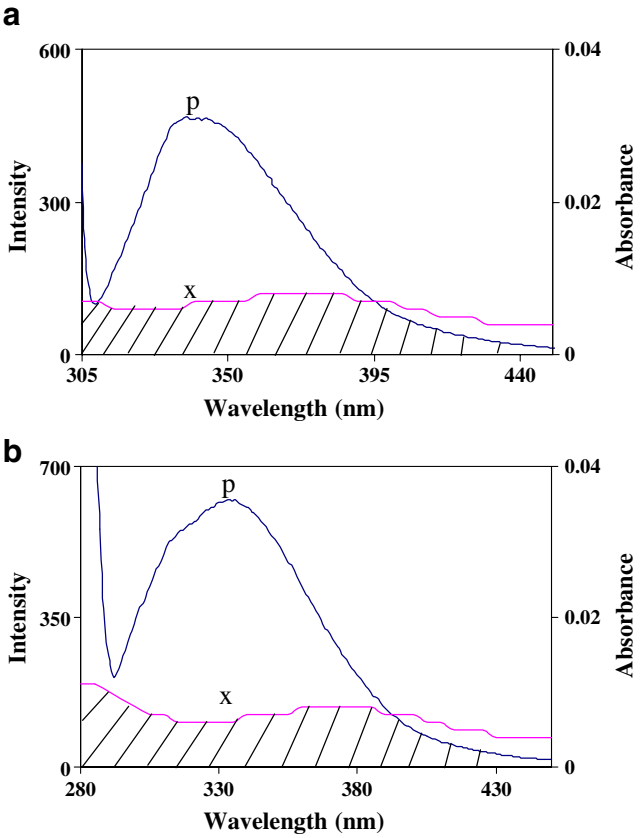

Fig. 8 The overlap of the UV absorption spectrum of drug (x) with fluorescence spectrum of protein (p); equimolar concentration (1.237 μM) of drug and protein were used (**a**) LXM-BSA and (**b**) LXM-HSA system

where F_0 and F are the fluorescence intensities without and with LXM, r is the binding distance between donor and acceptor, and R_0 is the critical distance when the efficiency of energy transfer is 50%. The value of R_0 can be calculated using the equation shown below:

$$R_0^6 = 8.79 \times 10^{-25} k^2 n^{-4} \phi J \tag{8}$$

where k^2 is the spatial orientation factor between the emission dipole of the donor and the absorption dipole of the acceptor, n is the refractive index of the medium, $ø$ is the fluorescence quantum yield of the donor and J is the overlap integral of the fluorescence emission spectrum of the donor and the absorption spectrum of the acceptor and is given by

$$\Delta J = \frac{\sum F(\lambda)\varepsilon(\lambda)\lambda^4 d(\lambda)}{\sum (F(\lambda)d(\lambda)} \tag{9}$$

where $F(\lambda)$ is the corrected fluorescence intensity of the fluorescent donor at wavelength, λ and $\varepsilon(\lambda)$ is the molar absorption coefficient of the acceptor at wavelength, λ.

For HSA, k^2=2/3, n=1.336, ε=0.118 and for BSA, k^2=2/3, n=1.336, ε=0.15 [33]. It was experimentally found that $J=1.301\times10^{-15}$ cm^3Lmol^{-1}, R_0=1.95 nm, E=0.23, r=2.38 nm for LXM-BSA and $J=1.235\times10^{-15}$ cm^3 $Lmol^{-1}$, R_0=2.08 nm, E=0.23, r=2.56 nm for LXM-HSA, respectively. The donor-to-acceptor distance less than 8 nm indicated that the energy transfer from BSA/HSA to drug occurred with high probability [34].

Effects of K^+, Ca^{2+}, Cu^{2+} and Zn^{2+} on Binding of LXM with BSA/HSA

The effects of some common ions on the binding of LXM with BSA/HSA was investigated at 294 K by recording the fluorescence intensity in the range of 300–450 nm upon excitation at 296/280 nm. Under the experimental conditions, no cations gave precipitate in phosphate buffer. It is evident from Table 3 the K values were either increased or decreased in presence of certain cations. The higher binding constant values might have been resulted from the interaction of cation with drug to form a complex, which in turn interacted with protein. From the pharmacokinetics perspective, the increase in the binding constant will buffer the drug concentration in the blood and prolong the duration in plasma [34, 35]. Hence, maximum effectiveness of the drug will be achieved. However, decrease in the binding constant of LXM-HSA results in LXM to be quickly cleared from the blood, which may lead to the need for more doses of LXM to achieve the desired therapeutic effect [35, 36].

Conclusions

This paper provided an approach for studying the interactions of fluorescent plasma protein with LXM using absorption, fluorescence, FT-IR and circular dichroism techniques for the first time. We have investigated the interactions of LXM with BSA/HSA as the binding (of the drug to serum albumins) influences the drug availability at the site of action. LXM quenched the fluorescence of BSA/HSA through dynamic quenching mechanism. The distance between the donor (protein) and the acceptor (LXM) was also calculated using FRET. The biological significance of this work is evident since albumin serves as a carrier molecule for multiple drugs and the interactions of LXM with albumins are not characterized so far. Hence, this report has a great significance in pharmacology and clinical medicine as well as methodology.

Table 3 Effects of common ions on binding constants of LXM-BSA and LXM-HSA at 294 K

Metal ion	K for LXM-BSA (M^{-1})	K for LXM-HSA (M^{-1})
K^+	2.44×10^5	8.98×10^3
Ca^{2+}	1.83×10^5	5.70×10^3
Cu^{2+}	1.22×10^5	3.44×10^3
Zn^{2+}	1.20×10^5	1.15×10^5

Acknowledgements The financial support of the CSIR, New Delhi (No. 01(2279)/08/EMR-II dated 20-11-2008) is gratefully acknowledged. We are thankful to Head, Molecular Biophysics, Indian Institute of Science, Bangalore, for CD measurement facilities. Thanks are also due to the authorities of the Karnatak University, Dharwad, for providing necessary facilities.

References

1. Xiao J, Shi J, Cao H, Wu S, Ren F, Xu M (2007) Analysis of binding interaction between puerarin and bovine serum albumin by multi-spectroscopic method. J Pharm Biomed Anal 45 (4):609–615
2. He W, Li Y, Xue C, Hu Z, Chen X, Sheng F (2005) Effect of Chinese medicine alpinetin on the structure of human serum albumin. Bioorg Med Chem 13(5):1837–1845
3. Sułkowska A, Maciazek M, Równicka J, Bojko B, Pentak D, Sułkowski WW (2007) Effect of temperature on the methotrexate-BSA interaction: Spectroscopic study. J Mol Struct 834–836, 162–169
4. Zhang G, Wang A, Jiang T, Guo J (2008) Interaction of the irisflorentin with bovine serum albumin: a fluorescence quenching study. J Mol Struct 891(1–3):93–97
5. Tian J, Liu J, Tian X, Hu Z, Chen X (2004) Study of the interaction of kaempferol with bovine serum albumin. J Mol Struct 691(1–3):197–202
6. Y-J Hu, O-Yang Y, Bai A-M, Li W, Liu Y (2010) Investigation of the interaction between ofloxacin and bovine serum albumin: spectroscopic approach. J Solution Chem 39(5):709–717
7. Mote US, Bhattar SL, Patil SR, Kolekar GB (2010) Interaction between felodipine and bovine serum albumin: fluorescence quenching study. Luminescence 25(1):1–8
8. Subramanyam R, Gollapudi A, Bonigala P, Chinnaboina M, Amooru DG (2009) Betulinic acid binding to human serum albumin: a study of protein conformation and binding affinity. J Photochem Photobiol B 94:8–12
9. Varlan A, Hillebrand M (2010) Bovine and human serum albumin interactions with 3-carboxyphenoxathiin studied by fluorescence and circular dichroism spectroscopy. Molecules 15:3905–3919
10. Neelam S, Gokara M, Sudhamalla B, Amooru DG, Subramanyam R (2010) Interaction studies of coumaroyltyramine with human serum albumin and its biological importance. J Phys Chem B 114:3005–3012
11. He W, Chen H, Sheng F, Yao X (2009) Molecular modeling and spectroscopic studies on binding of 2, 6-bis[4-(4-amino-2 trifluoromethylphenoxy)benzoyl] pyridine to human serum albumin. Spectrochim Acta Part A 74(2):427–433
12. Silva D, Cortez CM, Cunha-Bastos J, Louro SRW (2004) Methyl parathion interaction with human and bovine serum albumin. Toxicol Lett 147(1):53–61
13. Yuan T, Weljie AM, Vogel HJ (1998) Tryptophan fluorescence quenching by methionine and selenomethionine residues of calmodulin: orientation of peptide and protein binding. Biochemistry 37(9):3187–3195

14. Yue Y, Chen X, Qin J, Yao X (2009) Spectroscopic investigation on the binding of anti neoplastic drug oxaliplatin to human serum albumin and molecular modeling. Colloids Surf, B 69(1):51–57
15. Lemma T, Pawliszyn J (2009) Human serum albumin interaction with oxaliplatin studied by capillary isoelectric focusing with the whole column imaging detection and spectroscopic method. J Pharm Biomed Anal 50(4):570–575
16. Lakowicz JR (1999) Principles of fluorescence spectroscopy, 2nd edn. Kluwer/Plenum, New York
17. Sarkar D, Mahata A, Das P, Girigoswami A, Ghosh D, Chattopadhyay N (2009) Deciphering the perturbation of serum albumins by a ketocyanine dye: a spectroscopic approach. J Photochem Photobiol B Biol 96(2):136–143
18. Sudlow G, Birkett DJ, Wade DN (1976) Further characterization of specific drug binding sites on human serum albumin. Mol Pharmacol 12(6):1052–1061
19. Peters T (1995) All about albumin; biochemistry, genetics and medical applications. Academic, San Diego
20. Gerbanowski A, Malabat C, Rabiller C, Gueguen J (1999) Grafting of aliphatic and aromatic probes on rapeseed 2*S* and 12*S* proteins: influence on their structural and physicochemical properties. J Agric Food Chem 47(12):5218–5226
21. Daneshgar P, Akbar A, Movahedi M, Norouzi P, Ganjali MR, Sobhani AM, Saboury AA (2009) Molecular interaction of human serum albumin with paracetamol: spectroscopic and molecular modeling studies. Int J Biol Macromol 45(2):129–134
22. Förster T (1965) In: Sinanoglu O (ed) Modern quantum chemistry. Academic, New York
23. Yu Z, Li D, Ji B, Chen J (2008) Characterization of the binding of nevadensin to bovine serum albumin by optical spectroscopic technique. J Mol Struct 889(1–3):422–428
24. Lu ZX, Cui T, Shi QL (1987) Applications of Circular Dichroism and Optical Rotatory Dispersion in Molecular Biology, 1st edn. Science Press
25. Kang J, Liu Y, Xie MX, Li S, Jiang M, Wang YD (2004) Interactions of human serum albumin with chlorogenic acid and ferulic acid. Biochim Biophys Acta 1674(2):205–214
26. Wang Y, Tang B, Zhang H, Zhou Q, Zhang G (2009) Studies on the interaction between imidacloprid and human serum albumin: spectroscopic approach. J Photochem Photobiol B Biol 94(3):183–190
27. Sahoo BK, Ghosh KS, Dasgupta S (2008) Investigating the binding of curcumin derivatives to bovine serum albumin. Biophys Chem 132(2–3):81–88
28. Mandeville JS, Froehlich E, Tajmir-Riahi HA (2009) Study of curcumin and genistein interactions with human serum albumin. J Pharm Biomed Anal 49(2):468–474
29. Mandal P, Ganguly T (2009) Fluorescence spectroscopic characterization of the interaction of human adult hemoglobin and two Isatins, 1-Methylisatin and 1-Phenylisatin: a comparative study. J Phys Chem B 113(45):14904–14913
30. Zhoua J, Wu X, Gu X, Zhou L, Song K, Wei S, Feng Y, Shen J (2009) Spectroscopic studies on the interaction of hypocrellin A and hemoglobin. Spectrochim Acta Part A 72(1):151–155
31. Grigoryan KR, Aznauryan MG, Bagramyan NA, Gevorkyan LG, Markaryan SA (2008) Spectroscopic determination of binding between human serum albumin and a platinum (II) dimethylsulfoxide complex. J Appl Spectrosc 75(4):593–596
32. Stryer L (1978) Fluorescence energy transfers as a spectroscopic ruler. Annu Rev Biochem 47:819–846
33. Cyril L, Earl JK, Sperry WM (1961) Biochemists handbook. E & FN Epon Led, London
34. Sun Y, Zhang H, Sun Y, Zhang Y, Liu H, Cheng J, Bi S, Zhang H (2010) Study of interaction between protein and main active components in Citrus aurantium L. by optical spectroscopy. J Lumin 130(2):270–279
35. Khan SN, Islam B, Yennamalli R, Sultan A, Subbarao N, Khan AU (2008) Interaction of mitoxantrone with human serum albumin: spectroscopic and molecular modeling studies. Eur J Pharm Sci 35(5):371–382
36. Cuia F, Qin L, Zhanga G, Liu Q, Yao X, Lei B (2008) Interaction of anthracycline disaccharide with human serum albumin: investigation by fluorescence spectroscopic technique and modeling studies. J Pharm Biomed Anal 48(3):1029–1036